[5] Paterson, R. W., "Turbulent Flow Drag Reduction and Degradation with Dilute Polymer Solutions," TR Contract N00014-67-A-0298-0002, 1969, Harvard Univ., Cambridge, Mass.

[6] Whitsitt, N. F., Harrington, L. J., and Crawford, H. R., "Effect of Wall Shear Stress on the Drag Reduction of Viscoelastic Fluids," *Viscous Drag Reduction*, edited by C. S. Wells, Plenum Press, 1969, p. 265.

[7] Goldstein, S., "On the Resistance to the Rotation of a Disc Immersed in a Fluid," *Proceedings of the Cambridge Philosophy Society*, Vol. 31, 1935, p. 232.

[8] Deb, S. D. and Mukherjee, S. N., "Molecular Weight and Dimensions of Guar Gum from Light Scattering in Solution," *Indian Journal of Chemistry*, Vol. 1, 1963, p. 413.

[9] Hoyt, J. W. and Fabula, A. G., "The Effect of Additives on Fluid Friction," TR 3670, 1964, U.S. Naval Ordnance Test Section, China Lake, Calif.

[10] Richter, J., "Effect of Guar-Gum in Water on Flow through a Pipe," M.S. thesis, 1967, Dept. of Hydraulics and Mechanics, Univ. of Iowa, Iowa City, Iowa.

[11] Hung, T. C., "Effect of High Polymer Additives in Turbulent Flow," M.S. thesis, 1968, Dept. of Hydraulics and Mechanics, Univ. of Iowa, Iowa City, Iowa.

[12] Miloh, T., "Boundary Layer on a Disc Rotating in Dilute Polymer-Solution," M.S. thesis, 1969, Dept. of Civil Engineering, Technion, Israel Institute of Technology, Israel.

[13] Fabula, A. G., Lumely, J. L., and Taylor, W. D., "Some Interpretations of the Toms Effect," paper presented at the Syracuse University Rheology Conference, Soranoe Lake, N. Y., Aug. 1965.

APRIL 1971 J. HYDRONAUTICS VOL. 5, NO. 2

An Experimental Study of Turbulent Diffusion of Drag-Reducing Polymer Additives

R. R. WALTERS* AND C. S. WELLS†
Advanced Technology Center, Inc., Dallas, Texas‡

An experimental study of the mechanics of turbulent diffusion when uniformly injecting a drag-reducing polymer solution through a wall adjacent to a fully developed pipe flow of water is described. Experimental diffusion data were obtained using very low injection rates in a porous wall pipe test section designed on the basis of a prior theoretical diffusion analysis with uniform injection. The drag-reducing effectiveness of the polymer only in the wall region, discovered previously, is substantiated by detailed concentration profile, velocity profile and wall shear stress data. These data indicate that an increase in the viscous sublayer thickness is accompanied by an increase in the diffusion sublayer thickness for uniform drag-reducing polymer injection. Also, uniform polymer injection at the wall appeared to somewhat inhibit the turbulent diffusion away from the wall. This type of injection provided drag reduction with a much smaller supply of polymer than required to raise the concentration throughout the shear layer to the same drag-reducing level.

Nomenclature

A_i = active porous wall injection area
ΔB = defined by Eq. (1) using f based on pressure drop only
c = time averaged local concentration of injected tracer in the stream, ppb
c_i = concentration of injected tracer at the wall, ppb
$\bar{c}_{\mathrm{INT}}$ = integrated average bulk concentration of tracer in the stream, ppb
$\bar{c}_m$ = measured average bulk concentration of tracer in the stream, $(\dot{m}_i/\dot{m}_t)(c_i)$, ppb
$\bar{c}_p$ = measured bulk concentration of the polymer in the mainstream, ppm, $(\dot{m}_i/\dot{m}_t)X$ (concentration of polymer injection solution)
c^+ = dimensionless concentration variable, $\rho(1 - c/c_i)u_*/(\dot{m}_i/A_i)$
D = tube diameter, $2R$
$\mathfrak{D}_w$ = molecular diffusion coefficient defined in terms of conditions at the wall
f = friction factor, defined as $(R/\rho\bar{u}^2)(dP/dx)$
g = gravitational constant
$\dot{m}_i$ = total mass flow rate (mass/unit time) injected through the porous wall $(\dot{w}_i/g)$
$\dot{m}_t$ = mass flow rate of mainstream and injection fluid, $(\dot{w}_t/g)$
P = static stream pressure
R = tube radius
Sc = Schmidt number, $\nu_w/\mathfrak{D}_w$
u = local streamwise velocity
u_1 = stream velocity at tube centerline
u_* = shear velocity $(\tau_w/\rho)^{1/2}$
$\bar{u}$ = average bulk stream velocity
u_L = stream velocity at edge of viscous sublayer
u^+ = dimensionless velocity variable, u/u_*
$\dot{w}_i$ = total weight flow rate injected through the porous wall
$\dot{w}_t$ = weight flow rate of mainstream and injection fluid
x = streamwise spatial coordinate measured from upstream end of porous wall A
x' = streamwise distance from downstream end of last active porous wall to sampling probe
y = radial distance from wall of tube
y^+ = dimensionless wall distance variable, yu_*/ν_w
ν_w = kinematic viscosity at the wall
ρ = density of mainstream fluid
ρ_i = density of injected fluid
τ_w = shear stress at the wall, $(R/2)(dP/dx)$
Re = Reynolds number, $\bar{u}D/\nu_w$

Received August 27, 1970; revision received December 30, 1970. This research was supported by the Office of Naval Research under Contract N00014-69-C-0214 (Mathematical Sciences Division, Fluid Dynamics Program).

* Research Scientist, Aerophysics Group. Member AIAA.
† Senior Scientist, Aerophysics Group. Member AIAA.
‡ Formerly the LTU Research Center.

Introduction

THIS study was initiated to experimentally investigate the mechanics of turbulent diffusion when uniformly injecting a drag-reducing polymer solution through a wall adjacent to a fully-developed pipe flow of water. During this study, experimental diffusion data were obtained using a porous wall pipe test section and were 1) analyzed to obtain a more complete physical understanding of this type of diffusion, 2) compared with an analysis of turbulent diffusion for uniform drag-reducing polymer injection by Wells,[1] and 3) used as an analogue for the ablation of a solid polymer coating.

The turbulent diffusion analysis by Wells[1] resulted in an expression for determining the magnitude of the distributed mass flux of a drag-reducing polymer required at the wall to maintain significant drag reduction. This analysis is based on the assumption that the drag-reducing polymer need only be present in the wall region as opposed to the total shear layer. Recent tests in this laboratory had shown that an additive is effective in reducing drag only when it is present in the region near the wall, either in the viscous sublayer or in the buffer region.[2]

Numerous experimental data obtained under laboratory conditions for slot injection, such as in Ref. 2, have since appeared in the open literature; however, a significant void exists in the experimental diffusion data for the case of distributed mass transfer of a polymer from the wall. The effect of the polymer additive on the viscous sublayer and the corresponding effect of the sublayer on the reduction of wall friction can be determined by maintaining a distributed high polymer concentration at the wall only. This type of study is of interest for the application of a drag-reducing coating on external flow surfaces where the fluid mechanics of maintaining a non-Newtonian drag-reducing fluid in the wall region, whereas a Newtonian fluid exists in the outer turbulent region, needs to be better understood.

A pipe flow apparatus was chosen for these experiments because of the ease of controlling the test conditions. Calculations showed that the $\frac{3}{4}$-in. diam pipe used was not subject to the minimum pipe diameter effect described in Ref. 3. The results of turbulent shear flow in a pipe can be generalized to predict effects for external boundary layers, if significant effects are confined to the inner layer, rather than the outer layer, which is the substantial mixing region for external boundary layers, but is absent from pipe flow. The region of interest for uniform injection is the inner layer. The work described here can be distinguished from the study described in Ref. 4, which was primarily concerned with diffusion (dilution) far downstream of point injection of a polymer solution, where the concentration gradient was zero for values of the law of the wall variable, y^+ less than about 5000, and the mixing was confined to the outer layer.

Experimental Apparatus

A porous wall injection system was constructed to experimentally determine the mass flux at the wall of a drag-reducing polymer additive as a function of friction factor, velocity, and area of the porous wall, while measuring the velocity and concentration profiles. The design requirements were based on a prior parametric study using the diffusion analysis of Ref. 1. A porous wall material was selected from a set of commercially available specimens on the basis of 1) low polymer degradation due to passage through the porous material, 2) low filtration of the tracer element (Rhodamine B) and the polymer additive, 3) the ability to maintain a required mass flux with the available driving pressure, 4) pressure drop across the wall being an order of magnitude greater than the streamwise pressure drop to insure uniform injection over the surface of the porous wall, and 5) minimal hydraulic roughness on the stream side of the porous wall.

The porous wall injection system consists of three seamless, sintered stainless steel, smooth cylinders with an average pore size of 5 μ and integrated in a series arrangement into an existing $\frac{3}{4}$-in. pipe flow facility described in Ref. 5. Each porous cylinder has a wall thickness of $\frac{1}{4}$ in. and is 6 in. long with an inside diameter matching the existing test pipe. The porous cylinders were manufactured by Mott Metallurgical Corp. from Mott Series "A-5" porous (316) stainless steel, which has an approximate porosity of 40%. Chambers are built around each porous wall cylinder and supplied with fluid from a common reservoir, pressurized to force the injection solution into the boundary layer. The injection rate for each porous wall is controlled by an individual flowmeter. The flowmeters have an accuracy of $\pm 1\%$ of full scale, calibrated for both polymer solutions and water. The flowmeters and injection fluid reservoir air pressure regulation system are located on the injection control panel. The porous walls are held in place with $\frac{1}{2}$-in. wide Plexiglas spacers with a static pressure tap in each so that the streamwise pressure drops across each porous section can be measured. The porous cylinder and Plexiglas spacer combination forms a continuous smooth inside surface. All connections and facings are sealed with neoprene "O"-rings. A schematic of the porous wall sections is shown in Fig. 1.

Concentration profile and velocity profile measurements were made with a total head probe, 0.014 in. o.d. and 0.010 in. i.d., located in a probe holder immediately downstream of the porous wall sections for the tests reported herein. The local concentration measurements of the injection fluid in the mainstream was based on a fluorescein tracer solution mixed with the injection fluid and detected in the samples acquired at different radial distances from the wall. The samples were collected in small test tubes from a bleed hole in the exterior end of the total head probe. The tracer concentration in the samples was determined by means of a fluorometer. A Beckman Ratio Fluorometer, Model 772, was mounted in front of the control panel and was accurate in detecting tracer solution concentrations of two parts per billion.

As mentioned above, the porous wall apparatus was integrated with an existing $\frac{3}{4}$-in. pipe flow facility used in previous experiments in this laboratory. This facility is a blow-down type of system, which was used for these experiments to force water through the test pipe from a 400-gal reservoir maintained at a desired constant pressure head with air pressure regulators. The honed stainless steel test pipe has an inside diameter of 0.761 in. and a length of 224 in. Two $\frac{1}{32}$-in. diam static pressure taps, located two feet apart, the first of which was 151 diam from the tube entrance, were used for monitoring the upstream pressure drop as a check on the mass flow rate while changing the downstream porous wall injection rates. The first of the porous wall sections was connected to the downstream end of the 224-in. test pipe to insure fully developed turbulent flow at the entrance to the first porous wall section. A 50-in. long pressure drop section was located downstream of the three porous wall sections and the probe traversing mechanism to determine the variation in the pressure drop as the injection solution diffused into the mainstream. Therefore, pressure drop measurements for each run were made upstream of the porous walls, across each of the three porous walls and downstream of the porous walls. A total of five pressure drops could be measured with available instrumentation when taking a velocity profile measurement and seven pressure drop readings could be measured otherwise. The pressure taps were connected to a variable-reluctance transducer. The signal from the transducer was displayed on a digital voltmeter via a carrier amplifier. One of the pressure taps was connected to the total head probe for velocity profile measurements.

Flow rates of the mainstream were determined by using a weight tank at the exit water jet. The mainstream water was obtained from the local municipal water supply. The water temperature and injection fluid temperature were re-

corded for each run, as well as the viscosity for each polymer injection solution. Viscosities were measured with a Contraves viscometer using an MS-O concentric cylinder measuring system.

POLYOX(WSR-301), a poly(ethylene oxide) product of Union Carbide Corp., was used for all of the polymer injection data reported herein. The approximate molecular weight given by the manufacturer for this polymer is 4×10^6. The polymer solutions were mixed in 30-gal containers of local tap water by sifting the polymer powder into the wake of a 9-in. diam propeller turning at approximately 100 rpm. These solutions were covered and left undisturbed for 24 hr and then stirred for approximately five minutes before use.

The 500 ppm POLYOX solutions showed no tendency to clog the porous walls over the run time of approximately 15 min. However, a consistent increase in the main injection reservoir pressure was required to maintain a constant flow rate using 1000 ppm POLYOX solutions. The porous walls were easily back-flushed by opening the drain plugs on the porous wall reservoirs and using the available mainstream water pressure. The porous walls were flushed alternately in both directions with pure water for approximately 24 hr before recording water injection data after polymer injection tests had been made. Pressure drop data would then duplicate the original water injection data recorded before polymer injection.

Experimental Results

Initial Tests

Pressure drop and velocity profile measurements for pure water indicated fully developed turbulent smooth-wall pipe flow through the porous wall sections. However, at the highest velocity tested initially, 26 fps, a slight hydrodynamic roughness was indicated by the pressure drop measurements. In the preliminary experiments with polymer solution injection, measurements of the pressure drop across the porous wall sections and sections downstream confirmed that significant drag reduction could be obtained with the small mass injection rates predicted by the diffusion analysis of Ref. 1.

During these initial experiments, data were obtained for injection solutions of 100, 500, and 1000 parts per million of POLYOX(WSR-301) additive. A decrease in the streamwise pressure drop across each porous wall section and downstream sections was measured for each of the injection fluid concentrations as shown in Fig. 2 for the low injection to stream mass flux ratios indicated, except for the first active porous wall in some cases. The drag reduction is indicated here by positive values of the function ΔB.

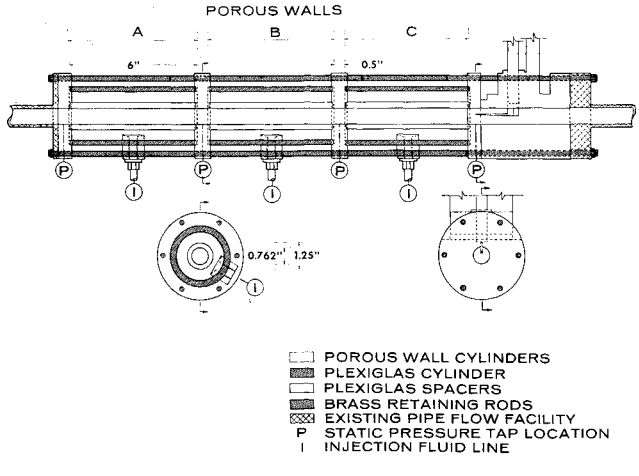

Fig. 1 Schematic of the porous wall injection system.

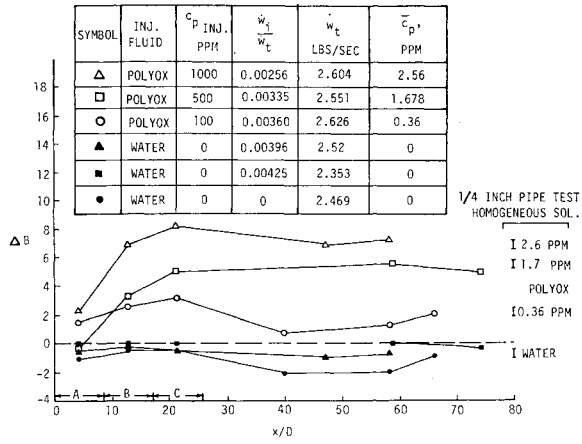

Fig. 2 Variation of local drag reduction for three different POLYOX solution concentrations and dimensionless downstream distance.

The following equation was used to calculate ΔB, that is,

$$\Delta B = (2)^{1/2}[(f)^{-1/2} - 4\log_{10}Re_w(f)^{1/2} + 0.39] \quad (1)$$

This relationship was used by Meyer[6] to correlate pressure drop data for polymer solutions with shear velocity u_*. The right side of the ΔB equation is equal to zero for values of f for smooth pipe flow of Newtonian fluids. In Fig. 2, ΔB is plotted vs the dimensionless downstream distance x/D, measured from the upstream end of the first porous wall section A.§ (For the $\frac{3}{4}$-in. pipe, $\Delta B = 8$ corresponds approximately to a 45% reduction in f, and $\Delta B = 4$ corresponds approximately to a 30% reduction in f.)

These data indicate that the amount of the drag reduction over the wall is very dependent on the polymer concentration of the injection fluid. The corresponding water data for each series of polymer data are also plotted in Fig. 2. The negative ΔB was attributed to a slight pipe roughness for the pipe configuration used downstream in the 100 ppm solution tests.

The pressure drop data obtained far downstream from the porous walls were compared with the variation of ΔB with concentration as determined from data obtained in a $\frac{1}{4}$-in. test pipe facility using small concentration homogeneous polymer solutions. This comparison in Fig. 2 shows good agreement between the data for the homogeneous polymer solutions and the data taken downstream ($x/D > 55$) in the $\frac{3}{4}$-in. pipe while injecting polymer in the upstream porous walls. The equivalent homogeneous solution bulk concentration in the $\frac{3}{4}$-in. pipe was determined by multiplying the injection concentration by the ratio of the injection to stream mass flux ($\dot{m}_i/\dot{m}_t$). The data from the $\frac{3}{4}$-in. and $\frac{1}{4}$-in. test pipes were compared at the same range of values for the shear velocity u_*, approximately equal to 0.5 fps.

A ratio of injection to stream mass flux for injection of water, greater than that used for the polymer injection, was tested with negligible evidence of boundary-layer displacement effects on the stream flow as indicated by velocity profile measurements. Also, the pressure drop data varied less than 5% over the range of water injection rates tested.

The injected polymer mass flux shown in Fig. 2 was controlled within 10% of the calculated optimum transverse mass flux through the shear layer predicted by the analysis of Ref. 1.

The expression resulting from this analysis which gives the transverse mass flux for drag-reducing fluids is

$$\dot{m}/(\rho u_1 A_i) = \frac{(f/2)(\bar{u}/u_1)^2(1 - c_1/c_w)}{1 + (u_L/u_*)(f/2)^{1/2}(\bar{u}/u_1)(Sc - 1)Sc^{-1/3}} \quad (2)$$

§ The porous wall sections are denoted as sections A, B, and C; A being the farthest upstream section, as shown in Fig. 1.

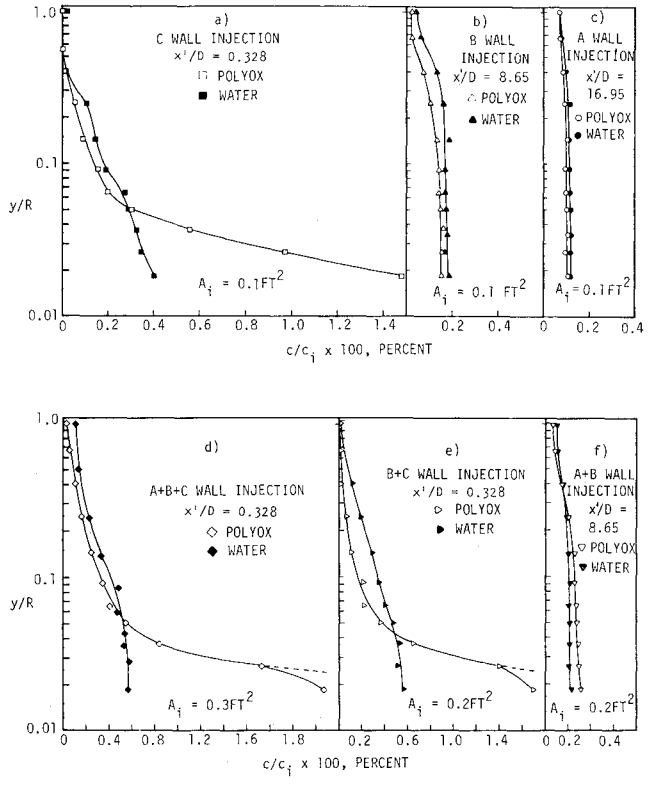

Fig. 3 Nondimensionalized concentration profiles comparing water and POLXOX injection for the six porous wall injection cases given in Table 1.

where c_l and c_w refer to the concentration at the centerline and wall, respectively. The Schmidt number (Sc) for water (or self-diffusion of most liquid solvents) is approximately 10^3 ($Sc \gg 1$), and $c_l/c_w \ll 1$ for these experiments. Therefore, Eq. (2) can be approximated by

$$\dot{m}/(\rho u_l A_i) = (f/2)^{1/2}(\bar{u}/u_l)/(u_L/u_*)(Sc)^{2/3} \qquad (3)$$

For homogeneous dilute solutions, u_L/u_* can be determined as a function of the flow conditions and the parameters of Meyer's correlation α and u_{*cr}, that is,

$$u_L/u_* - 5.75 \log_{10}(u_L/u_*) = 5.5 + \alpha \log_{10}(\bar{u}/u_{*cr})(f/2)^{1/2} \qquad (4)$$

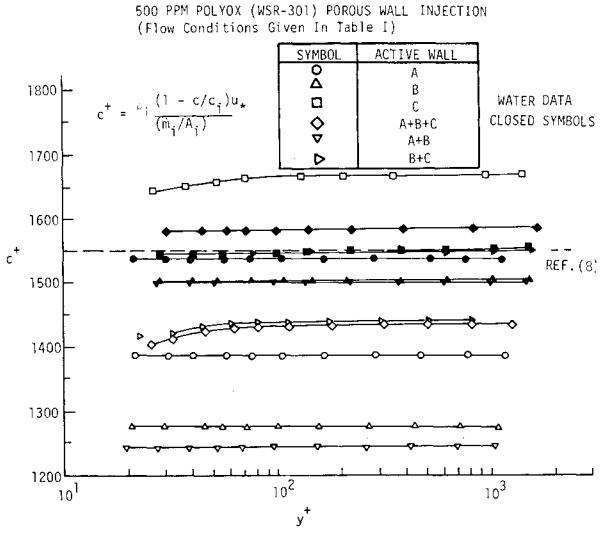

Fig. 4 Nondimensionalized concentration profile in the form of the law of the wall relationship.

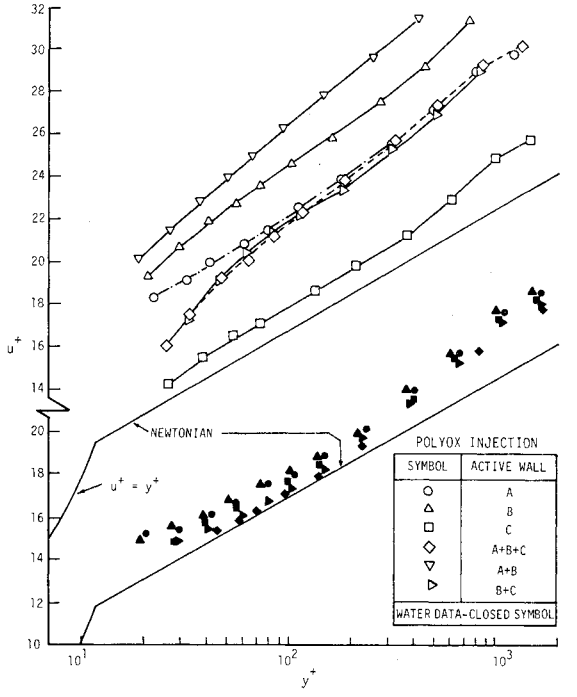

Fig. 5 Nondimensionalized velocity profiles in the form of the law of the wall for the six porous wall injection cases given in Table 1.

Eq. (4) is subject to the limitations of minimum pipe diameter and high-shear degradation described in Ref. 3. If a form of correlation other than Eq. (4) is appropriate, i.e., other than $\Delta B = \alpha \log_{10}(\bar{u}/u_{*cr})(f/2)^{1/2}$, the more general form,

$$u_L/u_* - 5.75 \log_{10}(u_L/u_*) = 5.5 + \Delta B \qquad (5)$$

can be used, where ΔB can be determined from Eq. (1), if the minimum pipe diameter criterion can be satisfied.

In order to use Eq. (3) to set $\dot{m}_i$ for a given $\bar{u}$, the experimental values of f for given injection conditions were used to calculate $\dot{m}_i$ and the injection rate was adjusted until experimental and calculated values were in rough agreement.

The Schmidt number was assumed here to be the same for the polymer solutions as for water. Although the authors are not aware of any experimental determinations of the molecular diffusion coefficient for dilute polymer solutions, this is believed to be a valid assumption due to the small changes in viscosity and implied negligible changes in thermal conductivity.[7]

Pressure drop data were obtained while varying the mass injection rate for three different velocities (7.5, 13, and 25 fps)

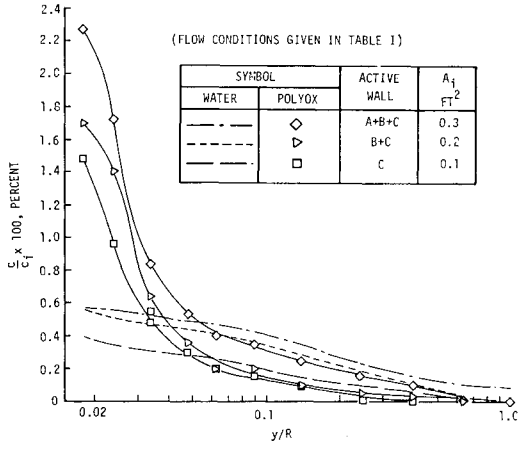

Fig. 6 Comparison of concentration profiles for variable upstream porous wall injection area.

Table 1 Experimental data associated with the six sets of concentration and velocity profiles for 500 ppm POLYOX solution and water injection in Fig. 3

GRAPHICAL SYMBOL	ACTIVE WALLS	INJECTION FLUID	$\frac{x'}{D}$	MAIN STREAM $\dot{w}_t$ LBS/SEC	MAIN STREAM $\bar{u}$ FT/SEC	$\bar{c}_m$ (MEASURED) PPB	$\bar{c}_{INT}$ (INTEGRATED) PPB	$\bar{c}_p$, PPM	INJECTION RATE $\dot{w}_i$ LBS/SEC	INJECTION RATE $\frac{\dot{w}_i}{\dot{w}_t}$
◇	A+B+C	POLYOX	0.328	2.490	12.66	26.46	22.60	1.325	0.0066	0.00265
◆	A+B+C	WATER	0.328	2.339	11.89	28.21	23.73		0.0066	0.00282
▽	A+B	POLYOX	8.65	2.500	12.69	17.60	18.47	0.880	0.0044	0.00176
▼	A+B	WATER	8.65	2.298	11.66	19.14	16.66		0.0044	0.00191
▷	B+C	POLYOX	0.328	2.469	12.53	17.82	12.06	0.891	0.0044	0.00178
▶	B+C	WATER	0.328	2.294	11.64	19.18	17.61		0.0044	0.00191
○	A	POLYOX	16.95	2.466	12.57	8.92	8.66	0.446	0.0022	0.00089
●	A	WATER	16.95	2.352	11.94	9.35	9.90		0.0022	0.00093
△	B	POLYOX	8.65	2.427	12.35	9.06	8.70	0.453	0.0022	0.00090
▲	B	WATER	8.65	2.312	11.73	9.51	13.14		0.0022	0.00095
□	C	POLYOX	0.328	2.407	12.21	9.14	9.85	0.457	0.0022	0.00091
■	C	WATER	0.328	2.298	11.66	9.57	8.86		0.0022	0.00095

for the three different polymer concentrations (100, 500, and 1000 ppm). From these optimization tests, a maximum reduction of the pressure drop readings across the porous wall sections was obtained for the 500 ppm POLYOX injection solution for the 13 fps average stream velocity ($\bar{u}$) at a value of $\dot{m}_i/\dot{m}_t = 0.0026$. This corresponds to a wall injection velocity to average stream velocity ratio equal to 6.8×10^5. The maximum pressure drop reduction was found for the 1000 ppm POLYOX injection solution at the 13 fps velocity at an $\dot{m}_i/\dot{m}_t$ of approximately 0.001. As a compromise between low concentration and effectiveness, detailed data were initially obtained using the 500 ppm POLYOX solution and are reported here. In general, the optimization tests showed that changing the concentration of the injected solution had a greater effect on pressure drop than changing the injection rate of a given solution.

Velocity and Concentration Profiles

As mentioned, the injection rate that produced a minimum pressure drop across the three porous walls was found to be about 0.022 lb/sec ft^2, for the medium velocity tested of 13 fps for the 500 ppm POLYOX(WSR-301) injection solution. These parameters were held constant while the velocity profile and concentration profile were obtained with a total head tube stationed immediately behind the third porous wall. These data were obtained for six different combinations of the three porous walls located in a series arrangement, in order to vary both the amount of injection area in front of the probe and the downstream distance from the injection area to the probe. The total head probe was located at the downstream end of the last injection section, porous wall C.

Concentration profile data are shown in Figs. 3, 4, 6, and 7, and velocity profile data are given in Fig. 5.

The comparisons of all six concentration profiles for polymer injection vs water injection are shown in Figs. 3a–f, where the ratio of local concentration to injected concentration c/c_i is plotted vs dimensionless distance from the wall y/R. The data in Figs. 3b and 3c show that the concentration gradients and differences for water and polymer injection almost vanish within a distance of about 9 diam downstream from the end of porous wall injection. Even when the upstream injection area is doubled, this still appears to be true, as shown in Fig. 3f. The concentration profiles obtained immediately behind an active porous wall using polymer injection (Figs. 3a, 3d, and 3e) have a much larger change in concentration across the pipe than do the profiles for injection of water. The concentration profiles are plotted in Fig. 4 in the dimensionless form c^+ vs y^+, which can be shown to be the correct variables if both the velocity and concentration distribution are assumed to be linear in y very near the wall. An analysis by Deissler[8] in terms of these variables shows that the approximate limiting c^+ value of 1550, given by Deissler's analysis for $Sc = 1000$, is in good agreement with the present water data, as shown in Fig. 4. A change of slope in the concentration distribution here can be interpreted as characteristic of approaching the diffusion sublayer.

The diffusion analysis discussed in Ref. 1 can be used to show that the ratio of diffusion sublayer thickness to viscous sublayer thickness (ratio of extent of linear concentration profile to extent of linear velocity profile) is approximately

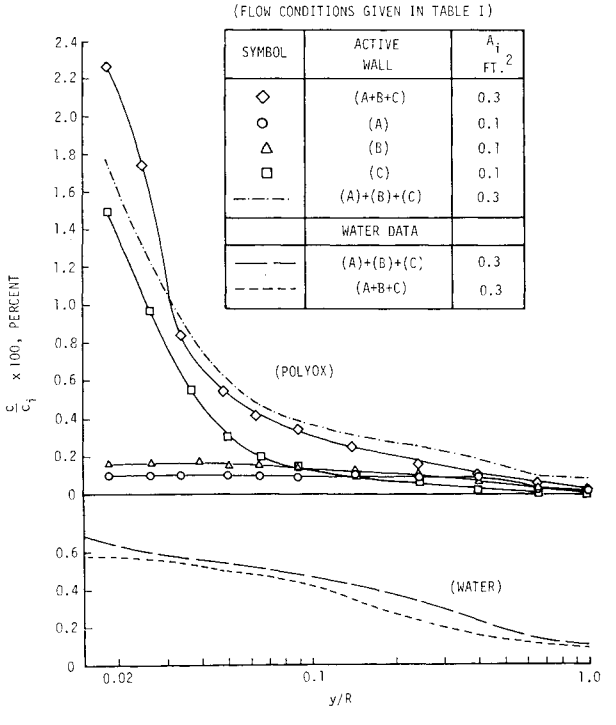

Fig. 7 Comparison of concentration profiles for single porous wall injection vs multiple porous wall injection.

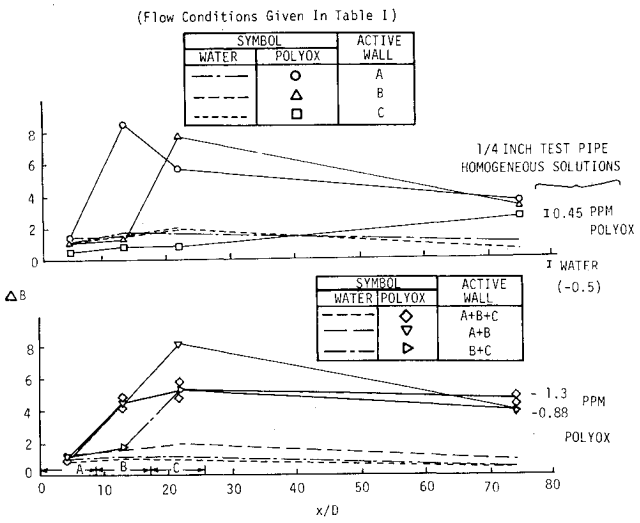

Fig. 8 Variation of drag reduction parameter (ΔB) based on pressure drop only over porous wall sections.

equal to $(Sc)^{1/3}$, which is about 10 for these fluids. Deissler's logarithmic concentration profile shows no deviation from constant c^+ for values of y^+ greater than about 5. Since the probe used in the present experiments could not measure closer to the wall than about $y^+ = 20$, no deviation from constant c^+ should be expected for the water injection data. This is seen in Fig. 4. However, it can be seen in Fig. 4 that the three concentration profiles taken immediately behind active porous wall injection of polymer solutions show a significant deviation from constant c^+ at a value of y^+ of about 100, or about a 20-fold increase in the distance from the wall over which the concentration changes greatly. Thus, the effect of the polymer in changing transport conditions near the wall and not in the turbulent core is seen in these diffusion experiments, as it has been observed in previous momentum transport experiments.

The corresponding velocity profiles are presented in Fig. 5 in terms of law of the wall parameters, u^+ and y^+. The universal velocity profile, or inner law is represented by[9]

$$u^+ = 5.75 \log_{10} y^+ + 5.5$$

using the empirical constants for smooth-wall Newtonian pipe flow. The water data are in good agreement with the above semilogarithmic expression. However, when the polymer solution was injected, the velocity profile shifted upward parallel to the Newtonian line, as is typical of drag-reducing fluid flows. Here a change in slope from that of the turbulent core region is characteristic of approaching the viscous sublayer. It can be seen that such a change in slope occurs for the three velocity profiles taken immediately behind an active porous wall section with polymer injection. Therefore, the concentration and velocity profiles obtained immediately behind an active porous wall with polymer injection characterize an increase in the diffusion sublayer thickness and the momentum sublayer thickness, respectively.

Figures 3a, 3d, and 3e are replotted in Fig. 6 to directly compare the differences in the water and polymer concentration profiles when only the injection area in front of the probe is changed. As shown in Fig. 6, an increase in the continuous injection length in front of the sampling probe station increased the measured concentration in the wall region to a greater extent than the region away from the wall, for the polymer injection. When the continuous injection area in front of the probe was doubled, the concentration was increased very significantly below $y/R = 0.1$, whereas the concentration for $y/R > 0.1$ changed insignificantly. Increasing the injection area by a factor of 3 increased the concentration over a greater part of the boundary layer; however, a significant increase was again measured near the wall. This can be contrasted with the case of increasing the continuous injection area for water; that is, when the area was increased, the concentration throughout the boundary layer was increased, including at the tube centerline.

The continuous length polymer injection, using all three porous walls, is compared to the summation of the three individual wall injections in Fig. 7 to indicate the change in diffusion found when using continuous polymer injection as opposed to a more localized injection. The dashed line in Fig. 7 is a summation of the concentration measurements of polymer injection at A only, B only, and C only. Maintaining a continuous high polymer concentration at the wall appears to inhibit the transverse mass transfer. The concentration of injection fluid in the measurable inner wall region did not increase over that in the region away from the wall for continuous water injection when compared with the summation of the local concentrations for individual porous wall water injection.

Drag Reduction Characteristics

The pressure drop data associated with the six different injection conditions corresponding to the concentration and velocity profiles are shown in Fig. 8. This plot of ΔB vs the dimensionless downstream distance, measured from the upstream end of the first porous wall, is calculated from the pressure drop measurements. The viscosity of the injection fluid (500 ppm POLYOX solution) evaluated at the wall shear stress, was used for the viscosity at the wall over the active injection sections. For the inactive porous walls and the other solid wall sections the viscosity of water was used. There was approximately a 30% change between the 500 ppm POLYOX solution viscosity and the water viscosity for the wall shear stress measured. This difference in viscosity changed the ΔB value by less than 0.5, according to Eq. (1).

As shown in Fig. 8, for the case of injection of the polymer solution through all three porous walls, the value of ΔB over section C is greater than over section B, which is in turn greater than over section A. The entrance length for both heat and mass transfer should be less than about 5 diam for Newtonian fluids with $Sc = 1000$ (Ref. 8). However, the diminished mass transport in the wall region for diffusion of polymer solutions apparently results in a longer entrance region. The greatest reduction in ΔB was recorded immediately behind the last active porous wall for both single wall injection and the multiple wall injection. The increased magnitude of ΔB occurring immediately behind the last active porous wall, greater than that for a homogeneous solution, is indicative of the effectiveness of the polymer in the region close to the wall. Figure 8 shows this effect across porous wall C for both the A + B injection case and the B injection case, and across porous wall B with injection at A only. Reviewing Fig. 3 for these cases shows consistently a relatively high polymer concentration near the wall immediately downstream of active sections and a relatively low uniform concentration downstream of inactive sections. That is, the profiles indicate a high wall concentration at the entrance of inactive sections immediately downstream of active sections, and an almost uniform concentration at the exit of those sections. The polymer concentration at each point can be determined by multiplying the c/c_i value by 500 ppm, the injected polymer concentration.

The resulting polymer concentration at the centerline for each of the above cases is not sufficient to promote the magnitude of pressure drop reduction seen across the sections under discussion. On the other hand, the high concentration measured at the closest approach of the probe to the wall, downstream of the active sections, does not result in large pressure drop reduction for those sections, as indicated in

Fig. 8. The ΔB data across the porous walls are well below the ΔB range of 22–25 measured in the $\frac{3}{4}$-in. pipe for a homogeneous solution at the injection concentration of 500 ppm used in these injection tests.

An attempt was made to determine the polymer concentration in the wall region from comparing $\bar{c}_m$ and $\bar{c}_{INT}$, by attributing the difference between the two to the remaining thin region close to the wall not considered in the integration of the concentration profile. However, the differences between $\bar{c}_m$ and $\bar{c}_{INT}$ for the position over the porous wall were about the same for the case of water injection as that for polymer injection, as shown in Table 1 (Table 1 is a summary of the flow and injection conditions for the experiments). Therefore, no concrete conclusions were derived from these comparisons; however, the diffusion sublayer is thinner than the viscous sublayer by a factor of about 0.1, and this tends to confine the high concentration solution to the region very near the wall. Conversely, Table 1 shows good agreement between $\bar{c}_m$ and $\bar{c}_{INT}$ for profiles measured downstream of inactive sections, which is a further confirmation of the uniform concentration extending to the wall.

Therefore, the data consistently show less reduction in pressure drop over active walls than can be inferred from the concentration profiles. Also, the reduction of pressure drop is greater over inactive sections downstream of active sections than over the active sections. Likewise, the concentration profiles show: 1) the injected polymer solution is held in the wall region ($y^+ < 150$) of active sections while injected water is diffused rapidly from the wall, and 2) both water and polymer solutions diffuse to an almost uniform profile over the length of an inactive section. The reason for the difference in pressure drop reduction over active and inactive sections cannot be determined absolutely from these data, but two explanations appear to be possible. Either 1) the polymer solution has not diffused far enough into the shear layer to give maximum drag reduction over the length of porous wall used; or 2) an anomalous effect of polymer injection is causing an increase in pressure drop that does not reflect the actual change in wall shear stress; i.e., the wall shear stress is reduced more than indicated by the pressure drop.

The former possibility is contrary to a great deal of other evidence that the concentrations measured in the wall region should produce a greater reduction in wall shear stress than the measured pressure drop reduction Further, the enhanced pressure drop reduction immediately downstream of active sections, when compared with the concentration profiles in that region, shows the effectiveness of the polymer in the wall region. And since the concentration in the downstream region is, near the wall, lower than over active sections, it would be expected that the reduction of pressure drop across active sections would be even larger, where the average concentration in the wall region is higher.

Therefore, the difference in pressure drop reduction over active sections and sections downstream of active sections suggests an anomalous pressure drop effect. In addition, the concentration profiles suggest that the anomalous effect is due to reduced mixing in the wall region, which causes a displacement effect. Even though the injection rate is very low, if the injected polymer solution does not mix with the incoming mainstream, the pressure drop could be significantly affected. An estimate of the effect of displacing the mainstream with the injected fluid yields an increase in pressure drop up to 20% of the Newtonian value. This is an indication that the pressure drop is not proportional to the wall shear stress if the injected fluid does not mix with the stream fluid.

Some very recent data also indicate this effect. Injection of a 1000 ppm solution shows the same trends of pressure drop over active and inactive walls. Injection of a 5000 ppm solution actually showed a 40% increase in pressure drop across the first active section and about a 70% reduction downstream of the active section. In both cases, when the

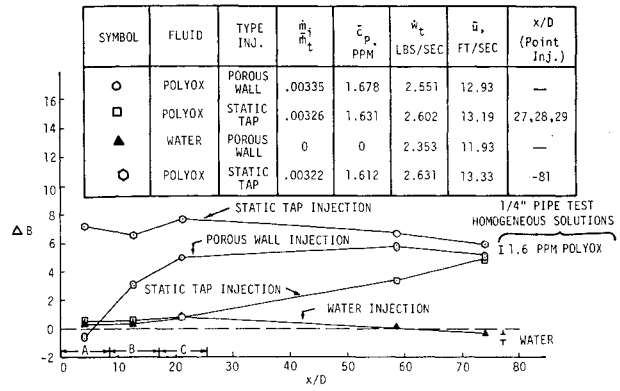

Fig. 9 Comparisons of downstream drag reduction for different injection configurations using a 500 ppm POLYOX injection solution.

injection rate was significantly reduced, the pressure drop across the first active section was also reduced.

Another possible cause of the anomalous pressure drop across the active section is a high viscosity at the wall. Recent comparison runs with injection of a high viscosity corn syrup solution (Newtonian) showed no effect on the pressure drop. However, this is not a positive indication of the absence of a viscosity effect in polymer solutions since the mixing, and therefore the concentration, in the wall region is greatly different for the two cases.

Recent tests have also shown that significant reductions in pressure drop can be found over active sections when injection rates even lower than the present values are used. This also tends to support the idea of displacement effects being responsible for the anomalous pressure drop, rather than viscosity.

In summary, the present data cannot be used to get quantitative indications of the reduction in wall shear stress over an active section because of the large reductions in mixing in the wall region. On the other hand, consistently large reductions in pressure drop downstream of active sections indicate the drag-reducing effectiveness of the polymer solution in the wall region at very low injection rates.

Further experiments are planned to investigate the anomalous effect on pressure drop, particularly with respect to obtaining maximum drag reduction over active sections, and determine the entrance length required to establish equilibrium drag reduction with uniform injection. Also planned are pressure drop and concentration profiles in the downstream vicinity of active sections to determine how quickly equilibrium is reached after termination of injection.

Polymer Degradation Tests

Tests were made to determine the amount of polymer degradation based on drag reduction effectiveness that was due to 1) shear, 2) passage through the porous wall injection section, and 3) configuration of the injection system. Part of a 500 ppm POLYOX(WSR-301) fresh solution was left untouched for a reference solution, part of the solution was passed through the porous wall only, at the highest injection rate used, and part of the solution was used to inject through the porous wall into a turbulent boundary layer at a known injection rate. The concentration of the homogeneous solution that existed at the $\frac{3}{4}$-in. test pipe exit was calculated to be 1.6 ppm. The untouched solution and the solution that passed through the porous wall only were diluted to this concentration.

Using the small $\frac{1}{4}$-in. test pipe apparatus, the drag reduction of the solution that was passed through the porous wall only was found to be approximately 4–5% less than that of the untouched reference solution. The solution that passed

through the porous wall and was subjected to a length of turbulent flow over 48 pipe diameters was found to be within 10% of the drag reduction measured in the $\frac{1}{4}$-in. test pipe for the reference solution.

The supply lines for the injection system were then connected to three pressure taps 81 diam upstream of the porous walls. The injection rate was the same as through the porous walls so that the concentration of the resultant homogeneous solution far downstream was identical to the previous concentration of 1.6 ppm. The results of these tests are shown in Fig. 9. Results of injection through three static taps—1, 2, and 3 in. downstream of the last porous wall section—are also shown. The injection was such that the resulting downstream concentration was the same as in the previous tests.

The drag reduction for all three cases at a section 74 diam downstream from the beginning of the porous walls agreed within 10%. The ΔB values for the upstream point injection case are slightly above the other two cases. The comparison of these tests with the homogeneous solution tests of the reference solution in the $\frac{1}{4}$-in. pipe is quite good. Also, the injection fluid and mainstream flow were thought to be fully mixed at the distance of 48 diam from the porous walls because of uniform pressure drop readings over consecutive sections and almost uniform concentration profiles after 9 diam from the porous wall polymer injection. Therefore, the far downstream pressure drop data, used to determine drag reduction, were assumed to be directly related to shear stress and not subject to the pressure drop anomalies in the vicinity of the porous wall discussed in the previous section.

The results of these tests indicate that for the flow conditions of these experiments there is approximately a 4–5% decrease in drag reduction effectiveness of the polymer due to its passage through the porous wall, and approximately a 10% decrease in drag reduction because of the over-all effect of passage through the porous wall and the turbulent shear layer. There is also approximately a 10% difference in drag reduction between distributed polymer injection and injection through a wall port. It is felt that this level of degradation is acceptable for the purposes of these experiments, since most of the significant conclusions are drawn from direct comparisons of drag reduction between various porous wall injection conditions.

The results of these tests for the different injection conditions are in excellent agreement with the downstream data of Fig. 8 for injection through all three sections, which resulted in about the same $\bar{c}_p$ value.

Conclusions

The following conclusions are presented, based on the foregoing presentation of data and subsequent discussion. 1) The porous wall apparatus adequately provides uniform injection of the polymer solution at very low injection rates and extremely low injection velocities, and provides for the study of the details of diffusion of polymer solutions from the wall region. 2) Turbulent diffusion is greatly reduced in the region near the wall ($y/R < 0.1$, $y^+ < 150$ for these experiments) with uniform injection of the polymer solution. This results in much higher concentrations very near the wall than for Newtonian diffusion. 3) The reduced mixing near the wall is reflected in both the velocity and concentration profiles, where the sublayer and buffer layer thicknesses for both momentum and mass transfer show significant increases over Newtonian values for uniform injection. This is consistent with earlier studies of polymer effects on transport of both momentum and heat. The relative shape of the velocity profiles for uniform injection appear to be more typical of those for high-concentration homogeneous solutions on the order of the injection concentration than for the low concentrations resulting from full mixing of the injected fluid with the stream. 4) Uniform injection provides drag reduction with a much smaller supply of polymer than required to raise the concentration throughout the shear layer to the same drag-reducing level. However, these experiments showed an anomalous pressure drop effect in the vicinity of the active injection sections. This was probably caused by displacement of the main stream by the great extent of reduced mixing in the region near the wall. 5) Further experiments are needed to obtain maximum drag reduction over the active injection sections, while minimizing the anomalous pressure drop effects. More detailed information on diffusion immediately downstream of uniform injection is also needed.

References

[1] Wells, C. S., "An Analysis of Uniform Injection of a Drag-Reducing Fluid into a Turbulent Boundary Layer," *Viscous Drag Reduction* (Proceedings of the Symposium in Dallas, Texas, Sept. 1968), Plenum Press, New York, 1969, pp. 361–382.

[2] Wells, C. S. and Spangler, J. G., "Injection of a Drag-Reducing Fluid into a Turbulent Pipe Flow of a Newtonian Fluid," *The Physics of Fluids*, Vol. 10, No. 9, Sept. 1967, pp. 1890–1894.

[3] Wells, C. S., "Use of Pipe Flow Correlations to Predict Turbulent Skin Friction for Drag-Reducing Fluids," *Journal of Hydronautics*, Vol. 4, No. 1, Jan. 1970, pp. 22–26.

[4] Fabula, A. G. and Burns, T. J., "Dilution in a Turbulent Boundary Layer with Polymeric Drag Reduction," TP 171, 1970, Naval Undersea Research and Development Center, Pasadena, Calif.

[5] Wells, C. S., Harkness, J., and Meyer, W. A., "Turbulence Measurements in Pipe Flow of a Drag-Reducing Non-Newtonian Fluid," *AIAA Journal*, Vol. 6, No. 2, Feb. 1968, pp. 250–257.

[6] Meyer, W. A., "A Correlation of the Frictional Characteristics for Turbulent Flow of Dilute Viscoelastic Non-Newtonian Fluids in Pipes," *AIChE Journal*, Vol. 12, No. 3, 1966, pp. 522–525.

[7] Wells, C. S., "Turbulent Heat Transfer in Drag-Reducing Fluids," *AIChE Journal*, Vol. 14, No. 3, 1968, p. 406.

[8] Deissler, R. G., "Analysis of Turbulent Heat Transfer, Mass Transfer and Friction in Smooth Tubes at High Prandtl and Schmidt Numbers," Rept. 1210, 1955, NACA.

[9] Schlichting, H., *Boundary Layer Theory*, 5th ed., McGraw-Hill, New York, 1960, p. 508.